FF

LBL-38599
UC-405
Preprint

Lawrence Berkeley Laboratory
UNIVERSITY OF CALIFORNIA

Submitted to *IEEE Transactions on Medical Imaging*

A Methodology for Specifying PET Volumes-of-Interest using Multi-Modality Techniques

G.J. Klein, X. Teng, W.J. Jagust, J.L. Eberling, A. Acharya,
B.W. Reutter, and R.H. Huesman

January 1996

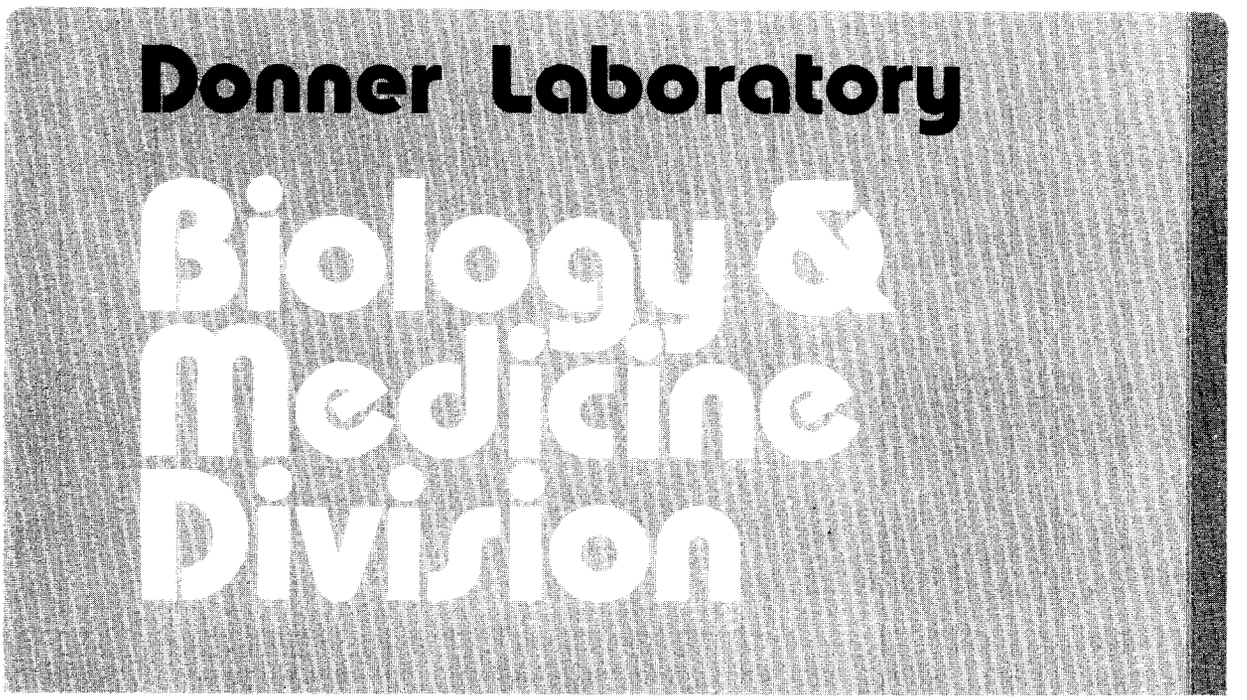

Prepared for the U.S. Department of Energy under Contract Number DE-AC03-76SF00098

A Methodology for Specifying PET Volumes-of-Interest using Multi-Modality Techniques*

GJ Klein, X Teng, WJ Jagust, JL Eberling, A Acharya,
BW Reutter and RH Huesman

Center for Functional Imaging
Lawrence Berkeley National Laboratory
University of California
Berkeley, CA 94720

* This work was supported in part by the Director, Office of Energy Research, Office of Health and Environmental Research, Medical Applications and Biophysical Research Division of the U.S. Department of Energy under contract No. DE-AC03-76SF00098 and in part by the U.S. Department of Health and Human Services under grants HL25840 , AG12435 and AG05890.

A Methodology for Specifying PET Volumes-of-Interest using Multi-Modality Techniques

GJ Klein, X Teng, WJ Jagust, JL Eberling, A Acharya,
BW Reutter and RH Huesman

Center for Functional Imaging
Lawrence Berkeley National Laboratory
University of California
Berkeley, CA 94720

Abstract

Volume of interest extraction for radionuclide and anatomical measurements requires correct identification and delineation of the anatomical feature being studied. We have developed a toolset for specifying 3D volumes-of-interest (VOIs) on a multislice Positron Emission Tomography (PET) dataset. The software is particularly suited for specifying cerebral cortex VOIs which represent a particular gyrus or mid-brain structure. A registered 3D magnetic resonance image (MRI) dataset is used to provide high-resolution anatomical information, both as oblique 2D sections and as volume renderings of a segmented cortical surface. VOIs are specified indirectly in 2D by drawing a stack of 2D regions on the MRI data. The regions are tiled together to form closed triangular mesh surface models which are subsequently transformed into the observation space of the PET scanner. Quantification by this method allows calculation of radionuclide activity in the VOIs as well as their statistical uncertainties and correlations. The methodology for this type of analysis and validation results are presented.

Key Words: Positron Emission Tomography, Volume-of-Interest, Brain, Multi-modality

1.0 Introduction

Quantitative analysis of multi-slice positron emission tomography (PET) datasets using regions of interest is a standard technique for studying brain function. A significant aspect of this technique is the process by which one identifies a desired portion of anatomy and then specifies its boundaries as a region of interest on a single slice, or a volume of interest (VOI) on a stack of slices. In particular, the availability of multislice scanners with true 3D imaging capabilities poses new challenges for 3D data analysis. Numerous issues related to this process exist which could skew quantitative results if not addressed properly. Because PET data represent functional, not necessarily anatomical

information, data from a PET scanner are not always appropriate for specifying regions. Functional boundaries seen on PET may not correlate with anatomical boundaries, hence, relying on these boundaries while specifying regions of interest could easily introduce quantification biases. Even where functional boundaries correspond to anatomical boundaries, the resolution obtained from the highest resolution PET scanners is often inadequate to confidently identify desired anatomical boundaries. For these reasons, many researchers have relied upon other modalities, such as Magnetic Resonance Imaging (MRI), to identify anatomy [1][2][3]. However, even with this multi-modality approach, the problem is not completely solved. Typical MRI datasets consist of 256x256x96 voxels and are usually displayed as 256x256 pixel images, one slice at a time. Trying to identify a region of anatomy, for example a particular gyrus in the cortex, from this slice-based data can be quite difficult even for experienced clinicians. Additional information is required to aid the 3D navigational task and to convey appropriate cues about the 3D nature of the anatomy.

In this paper, we describe a methodology for specifying meaningful 3D VOIs on PET datasets. The methodology is particularly suited for calculation of radiotracer activity and statistical uncertainty on cerebral cortex VOIs representing a particular gyral or deep brain structure. The approach addresses two problems that have plagued the specification of such regions in the past. First is the proper identification of a desired anatomical object from a functional PET image. Second is the specification of a true 3D boundary around that object once it is identified using conventional X-Windows interfaces. Unique in the approach is the method by which the regions can be used to accurately model statistical uncertainty of quantified activity in a 3D acquisition environment.

2.0 Methods

The procedure for obtaining quantitative PET VOI values can be summarized as follows. Our approach uses the high resolution anatomical data from MRI to identify and specify 3D regions of interest. The MRI data are registered to multislice PET data using a sequence of manual and automated techniques. VOI boundaries are specified on the MRI dataset by drawing 2D regions on a set of parallel image planes. The parallel set of planes may be chosen at any oblique slicing orientation through the MRI volume such that the cross sections most clearly show the features of the desired anatomical object. 2D regions are specified on these planes by drawing a freehand polygon or by laying out points which are then connected as a continuous cubic spline. Region drawing on this set of planes is facilitated by the display of a "3D cursor", which shows the position not only on the current drawing plane, but also on a number of slices orthogonal to the parallel planes, and on a volume rendering of a segmented cortical surface. Further feedback is provided by displaying the intersections of selected regions with these orthogonal slices

3D VOIs are formed by tiling each set of parallel 2D regions into a closed triangular mesh surface model. A matrix is calculated which describes the transformation between the registered MRI and PET, as well as between the

original and obliquely resliced MRI. This matrix is used to transform the surface model from the resliced MRI coordinate system into the coordinate system of the PET gantry. Once transformed, the VOI surface models may be used to calculate the activity within a 3D volume within the PET gantry. In our application, the surface models are currently projected onto the originally acquired PET slices, resulting in a series of labeled 2D regions. Quantification of activity within these regions and their uncertainty is achieved by projecting the regions into tomographic sinogram space, and then directly evaluating the counts in this space. Because the full region covariance matrix is available after this calculation, the 2D region values can be added together, giving an activity value and uncertainty for each PET VOI. Finally, VOI values are adjusted for the effects of partial volume by using the segmented MRI dataset as prior information.

Data referenced in this paper were acquired using a CTI- Siemens ECAT EXACT HR PET scanner and a 1 m bore 0.5 T Oxford MRI magnet with a home-built spectrometer. MRI volumes comprised a 3-dimensional data set of T1-weighted images (voxel size 1 x 1 x 2 mm, volume size 256 x 256 x 96 voxels) acquired using a 3-D gradient recalled echo sequence (TE = 14.3, TR = 30). PET data were obtained using the 47-slice scanner in 2D acquisition mode imaging the radiotracer, fluorodeoxyglucose (FDG). The data were reconstructed using standard 2D filtered backprojection techniques (voxel size 2.4 x 2.4 x 3.1 mm, volume size 128 x 128 x 47 voxels).

2.1 Segmentation/Registration

In order to relate MRI-based regions to PET measurements, it is necessary to spatially register the two datasets. Automated methods for this process exist but most require that the brain be segmented from non-brain regions in the MRI data[4][5]. Some have claimed success using completely automated methods to perform this segmentation. However, such techniques require special pulse sequences or complex clustering algorithms. We take a simpler approach relying on the facts that in FDG PET images, the outer cortex can be easily segmented from the background using image thresholding, and that the PET and MRI datasets can be approximately registered relatively quickly using manual techniques. As suggested by Pietrzyk [6], the registered and segmented PET data are used to mask the MRI and perform an automatic MRI segmentation. Once the segmented MRI is obtained, it is used to refine the PET registration via automatic techniques. Hence, the bulk of manual interaction that is required for the segmentation and registration exists solely in the "approximate" manual registration step.

Figure 1 shows the interface used to obtain a manual registration. Transverse, sagittal and coronal views of each dataset are simultaneously presented to a user, who is allowed to manipulate translation, rotation and scale parameters. The amount of misregistration is displayed via an interactive cursor showing corresponding points in the six views, or via an edge mask of either dataset which may be overlaid on the other set.

Once an approximate registration is found, the PET data are resliced at the resolution of the MRI volume and are thresholded to form a binary mask. To prevent slight misregistrations from masking away brain regions in the MRI, the PET mask is usually dilated using a morphological operator [7]. Further, to prevent masking the inner portions of the MRI brain, the outer boundaries of the PET mask are filled using a 2D filling operation. The resulting masked MRI dataset is a nearly complete segmentation; however, because the PET mask generally includes some portions of the outer tissue, a 3D region growing operation seeded from the interior of the cortex is used to obtain the final result. A final step in obtaining an accurate registration is the use of the segmented MRI dataset in an automated cross-correlation registration technique [4].

After registration and segmentation, an orientation file is stored which describes the registration parameters (nine parameters for rigid transformation with scaling). A 4x4 transformation matrix can be calculated from this orientation file, and it may be used to relate voxel positions in one volume to their corresponding positions in the resliced registered volume.

2.2 Volume of Interest Construction

2.2.1 Region Drawing Environment

Rather than attempting to create a sophisticated virtual reality environment for directly sculpting 3D VOIs, our approach uses conventional 2D X-Windows interfaces which indirectly specify surfaces through a sequence of 2D operations. That is, VOIs are constructed by drawing stacks of 2D regions. The region drawing environment makes use of two main principles to carry out this task. First, because the cross sectional 2D geometry of an object boundary can be considerably simplified just by reslicing along a different orientation, we allow the user to select a set of parallel slicing planes at angles different from the original acquisition planes. For cortical regions, the typical reslicing orientation is the coronal view of a transaxially acquired MRI. However, in general, these reslice orientations can be at any oblique angle with respect to the original acquisition orientation. Second, to aid in the 3D navigational task, simultaneous views of data are provided in different formats: volume rendered surfaces, orthogonal slices or registered PET slices, on which corresponding points can be visually related.

Figure 2 shows an example of the region drawing environment. Structured around the VIDA software package [8], a main window (Figure 2a), hereafter called the drawing plane, is provided for the user to draw 2D regions. Regions may be drawn using freehand polygons, laying out points connected via a cubic spline algorithm, or a number of other techniques. Any number of auxiliary viewing planes sliced at orthogonal angles (e.g. sagittal and coronal when the drawing plane is transverse) can be seen as well. A 3D cursor reflecting the position of the drawing cursor is projected on these views using a parallel projection technique. At any time, a keystroke may be hit while in the drawing plane to update the auxiliary views and display the orthogonal slices intersecting the current main cursor position

at that orientation. As a stack of 2D regions are drawn, their position with respect to one another may be displayed by showing the intersection with the auxiliary orthogonal planes (Figure 2b). Additionally, to provide guiding points while drawing regions on the drawing plane, curves may be drawn on the auxiliary views and their intersection with the drawing plane will be displayed.

For specifying cortical regions, probably the most useful visual cue is a rendering of the cortical surface. Historically, rendering techniques have been grouped into two subclasses, surface rendering and volume rendering. In surface rendering, a vector model is extracted from the underlying volumetric data, and is displayed as a set of shaded polygons. This technique has the advantage that it can take advantage of commonly available graphics hardware for real-time user interaction. It has the disadvantage that the process of extracting the polyhedral model can be extremely computationally intensive, and the model requires considerable storage to adequately describe a surface with enough detail. Volume renderings, on the other hand, are directly calculated from volume data and generally result in a single static image of one perspective of the shaded surface. An advantage of volume renderings is that high-quality renderings can be calculated quickly; however, once calculated, little interaction is possible because most of the 3D information has been lost.

We calculate volume renderings using a parallel projection gradient shaded technique on the segmented MRI data. Because a depth map calculated during the rendering is retained along with the corresponding transformation matrix, the 3D position of each point in the rendered surface can be calculated. Therefore, visual cues may be provided in two ways. First, a 3D polyline may be drawn on the rendering, and its intersections with the 2D drawing plane will be shown (Figure 3). This technique is useful for following a specific cortical gyrus through subsequent 2D slices. A second method provides real-time feedback between the drawing cursor and the volume rendering. As the cursor is moved in the drawing plane, its position in the rendering may be displayed as the projection of the cursor position along the line of sight used to obtain the rendering. Therefore, as the cursor is moved along the boundary of the cortex in the drawing plane, its correct position in the volume rendering is displayed.

2.2.2 VOI Construction

A typical set of 2D contours drawn for a brain dataset is seen in Figure 4a. Stacks of 2D ROIs like these could be used directly to calculate VOI statistics. This calculation could take place by summing voxels on calibrated PET images resliced at the same resolution and orientation of the MRI data. However, there are a number of advantages to constructing 3D surface models from the 2D stack, and describing them in a format independent of the discrete MRI voxel space, as depicted in Figure 4b. Here, the 2D regions are tiled together to produce VOI boundaries described as closed polyhedral surface models. These surface models can more smoothly represent slice-to-slice transitions than can discrete 2D stacks and can be easily manipulated for editing the overall 3D VOI shape and for transforming into other registered spaces.

For relatively simple regions, a graph-searching technique is suitable to produce acceptable tilings [9]. However, a more sophisticated tiling algorithm is required to prevent self-intersections in the tiled surface for complex cortical regions. We use the NUAGE [10] algorithm to obtain such tilings. This algorithm obtains a tiling based on a Delaunay triangulation of each 2D contour from which an exterior triangular surface is derived. To facilitate manipulations of the polyhedral surface model, the list of triangles is organized in a data structure known as a winged-edge structure [11]. This structure stores adjacency information between faces, vertices and edges and allows searches over these structures in linear time. The surface model is integrated into an Inventor Toolkit 3D graphical display environment [12]. In this environment, the user may visualize the resulting 3D region set and perform a number of arbitrary manipulations on them including scaling, translation and rotation, subdivision, selection and deletion.

2.3 PET Quantification

2.3.1 Statistical Quantification

As just stated, quantification of PET activity could take place directly using the stack of 2D regions by reslicing calibrated PET data into the voxel space of the MRI data. Of course, care must be taken to properly scale calibration factors in accord with the new voxel size of the resliced PET data, and to suitably treat voxels on the border of the region. Besides the error possibly induced from summing edge voxels, there is one main disadvantage to this technique: the uncertainty of the activity data can no longer be accurately characterized. If an accurate estimate of the activity within the region *and* its uncertainty are desired, calculations must take place in the observation space (i.e. projection, or sinogram space) of the tomograph, where the statistical properties are well established as a Poisson counting process [13],[14]. To carry out this calculation, the description of the VOIs must be transformed into the projection space of the PET scanner.

We acquire brain PET data as a set of 47 sinograms, one for each transverse plane, or slice, of the reconstructed PET volume. To obtain a suitable description of each VOI in projection space, the VOI is first transformed into the image space of the PET scanner using the 4x4 transformation matrix calculated during the PET-MRI registration and during the MRI reslicing processes. The 2D intersection of the VOI surface model with each acquisition plane is next calculated, resulting in another set of 2D regions. The uniformly-weighted interior of these regions is then forward projected into sinogram space, convolved with a ramp filter and the vector inner product with the attenuation-corrected emission counts is calculated. Complete knowledge of the covariance matrix between the 2D region values allows summing into composite values for each VOI, and calculation of their uncertainty. Values are computed as PET counts/sec/cc. Figure 5 summarizes the process.

Calculation of VOI activity by this method has a number of other advantages besides the capability of obtaining statistical properties. Since the high resolution anatomical data were used to define the VOI boundaries, the

PET data do not need to be greatly smoothed to obtain suitable visual image quality. Only a ramp filter is used, preserving spatial resolution during quantification. Also, because the technique effectively performs a fast reconstruction and summing of the data, reconstruction of a PET image volume is required only to register the data. For dynamic PET acquisitions, it is therefore not necessary to reconstruct every time point in the data acquisition. Finally, a third advantage is that calculation of VOI values for a 3D PET acquisition without septa would proceed in a straight-forward manner. In this case, a 2D forward projection of each VOI would be required at each projection angle, followed by convolution and calculation of the vector inner product.

2.3.2 Partial Volume Correction

Many have recognized the importance of correction for partial volume effects in PET quantification [15], [16]. The full width at half-maximum (FWHM) spatial resolution of the ECAT EXACT HR ranges from 3.6 mm to 7.4 mm throughout the field of view [17] whereas the dimension of typical structures of interest, such as cortical grey matter (5-7 mm), is well within this range. Activity calculated for a VOI drawn along the MRI-derived anatomical boundary of a uniformly active small cortical region is thus a considerable underestimate if the region is bordered by cerebrospinal fluid (CSF) or bone, which do not take up notable quantities of most radiotracers. Because the spatial resolution of MRI data is considerably higher than the PET resolution, we can account for this effect by using segmented MRI data to adjust the PET activity values. Ideally, if the spatial response of the PET scanner was known and one had access to an anatomical dataset perfectly segmented into regions of different uniform radiotracer uptake rates, for example grey matter, white matter, and CSF, the blurring could be completely deconvolved. Unfortunately, a reliable grey/white matter segmentation is difficult to obtain on a routine basis from typical clinical data obtained with a 0.5 T MR T1 acquisition, and quantification biases resulting from segmentation errors can be substantial. Up to a 20% error for a 2.82 mm missegmentation of the grey/white border has been reported [16] . For this reason, we take a simplified approach, segmenting the dataset into just two regions, brain and non-brain, and obtain a single factor for each region expressing the partial volume of non-brain region present in the VOI at the resolution of the PET scanner. Though this technique obviously suffers from the partial volume mixing of the grey and white matter, we feel that this error is less than may be incurred by using an unreliable trilevel segmentation.

The following procedure is used to obtain the partial volume factor. A segmented MRI dataset is registered and resliced into the reconstructed image space of the PET scanner at a resolution comparable to the MRI voxel size, thus avoiding potential aliasing effects during reslicing (2-3 times the voxel resolution of the reconstructed PET volume for our data). The segmented dataset is a binary indicator function of brain and non-brain regions seen in the MRI. To transform the resliced indicator function into the effective resolution of the PET scanner, the resliced MRI indicator mask is blurred to the resolution of the ECAT PET scanner using a 3D spatially-variant Gaussian convolution kernel derived from experimentally-determined resolution factors. These factors range from 3.6mm FWHM at

the center to 4.5 mm FWHM tangentially and 7.4 mm radially at R=20 cm, and from 4.0 mm FWHM at the center axially to 6.7 mm FWHM at R=20cm [17]. Because the tangential and radial components of the transaxial blur are approximately equal for radii which span the imaging location of the human head, the blurring is implemented as a 3-step 1D Gaussian convolution kernel. At each transaxial voxel location, the volume is first blurred using a kernel width in the X and the Y dimensions obtained by averaging the radial and tangential blur component at that location. Then the axial blur is carried out using the spatially-variant kernel in the Z direction. The Gaussian blur variance in all three directions is reduced by 1/6 of a voxel dimension to account for the blur already introduced by the resampling step. Summing the blurred indicator mask over the 3D extent defined by each VOI and dividing by the VOI volume gives a factor which compensates for the effects of partial volume.

3.0 Validation

A specific group of studies were performed in order to evaluate the procedures and software tools developed for analyzing three dimensional PET data. These experiments were performed in order to validate the region drawing, tiling, coregistration, and partial volume correction techniques.

3.1 Coregistration

An experiment was performed to compare the results of coregistration using an automated technique, the Automated Image Registration software package (AIR) [4] with a manual technique, the Multi-purpose Match (MPM) software package [6]. In addition, since the manual technique is operator dependent, we compared the results obtained by two different operators.

For these studies, 6 patients underwent MR and PET imaging. PET scanning was performed using an injection of approximately 10 mCi of fluorodeoxyglucose (FDG). Four of the patients had Alzhiemer's disease. These patients were selected because the PET images contained large irregular regions of hypometabolism which could potentially challenge automatic and manual registration methods.

After scans were obtained, the PET and MR images were coregistered with MPM using techniques described by its developers. For the AIR technique, MR images were manually segmented using region growing operations on a slice by slice basis to remove the skull and scalp. MR and PET were then coregistered automatically. The output from the AIR and MPM files were rewritten to a file format which described three parameters of translation and three parameters of rotation. These data were further reduced so that results could be compared on the basis of translational magnitude and rotational magnitude differences. These results are shown in Table 1. The registration accuracy is comparable to results reported by the developers of MPM [3] where accuracies within 1.84 mm for translation and 1.67 degrees for rotation were found.

3.2 Regions of Interest

A separate experiment was performed to determine the reliability of the procedure for reslicing volumetric data sets. An MRI scan was performed according to the aforementioned procedure in a normal young subject. A clearly delimited data set was produced from this by selecting 24 slices, thus limiting the dorsal and ventral extents of the dataset, and arbitrarily limiting the size of the data in three of the four transaxial directions using a masking feature. This resulted in a cubic region of brain, in which five of six sides were sharply delimited, and the sixth side was composed of the grey matter/cerebrospinal fluid (CSF) interface. Regions of interest were drawn to outline the entire brain area on the sequential 1 mm slices of brain, and the total volume of brain so enclosed was then determined. Subsequently, the data were resliced in the coronal plane and 33 1 mm thick slices were generated. Similar ROIs were drawn on these data in the coronal plane, and the volume of brain enclosed was also calculated. Volume for the original axial data was 29.1 ml and for the resliced data the volume was 28.3 ml, a difference of 2.8%.

A second experiment was performed to evaluate the effects upon calculation of regional cerebral metabolic rates for glucose (rCMRglc) of different methods of data analysis. Standard methods for computing rCMRglc, using regional PET activity, an arterial input function, and known rate constants with the operational equation were utilized [18] [19]. Two patients were studied. All ROIs were drawn on MR data. Six ROIs were drawn in each hemisphere of each patient, using predefined criteria for these regions (dorsolateral frontal cortex, orbital frontal cortex, anterior temporal cortex, posterior temporal cortex, amygdala, and hippocampus). Two different operators, each trained in neuroanatomy, drew these regions independently on data which had been resliced into a coronal plane (perpendicular to the line passing through the anterior and posterior commissures) using slices either every 1 mm or every 3 mm. Finally, the data were coregistered using either the MPM or AIR techniques. Thus, three different comparisons could be made: operator 1 vs. operator 2 ROIs, 1 mm resliced data vs. 3 mm resliced data, and manual vs. automatic coregistration. Comparisons were evaluated by calculating the rCMRglc for each brain region using each of the 8 possible methods and performing each comparison by collapsing across the other possible comparisons. Thus, a mean difference was calculated for each region for each comparison.

For the comparisons of operator 1 vs. operator 2, differences in rCMRglc across the 12 regions in the two patients ranged from 0.07% to 10.1% with an average difference of 3.7%. The greatest differences were found in the metabolic rates for the hippocampus, while most brain regions showed average differences on the order of 3-5%.

For comparisons of the manual vs. automatic methods of coregistration, rCMRglc differences ranged from 0.15% to 17%, with a mean difference of 5.5%. The greatest differences were found when values in orbital frontal cortex were compared. This brain region is particularly susceptible to errors in region placement since it is bordered anteriorly, superiorly, and inferiorly by bone and CSF.

For the comparisons between 1 mm and 3 mm resliced data, rCMRglc differences ranged from 0% to 7.3% with a mean difference of 1.9%. Except for one hemispheric hippocampal region in one subject with the highest percent difference, most differences were in the range of 1-3%.

3.3 Phantom Studies

In order to validate the methods developed for partial volume correction, a phantom was constructed to model three different intensities of MR signal or PET activity. The phantom consisted of a plexiglass cylinder divided into two compartments by a plexiglass wall. Through this wall, holes were drilled to permit passage of teflon tubing (3 mm internal diameter). Thus, the two plexiglass compartments could be filled with different fluids, and the tubing could be filled with a third fluid. This phantom was filled with water doped with copper sulfate for MR imaging. Compartment I was filled with water, compartment II was filled with copper sulfate-doped water, and the tubing was filled with a different copper sulfate doped water concentration to give MR signals that were sufficient for segmenting compartments in the resulting images. For PET imaging, compartment I was filled with water, compartment II with a solution of 5.9 μ Ci/ml and the tubing with a solution of 27.4 μ Ci/ml. Figure 6 shows a photograph of the plexiglass phantom.

Four sets of regions were drawn on the resliced MRI data, as is done in the routine analysis of brain data. Figure 7 shows slices through the originally acquired MRI and registered PET as well as VOIs projected onto the displayed transaxial slices of this dataset. Set A was a set of rectangular VOIs drawn completely within compartment II, set B was a set a of rectangular VOIs drawn on the right outer border of compartment II, set C was a set of rectangular VOIs drawn on the left outer border of compartment II, and set D was a set of cylindrical VOIs drawn over the 3mm tubes in compartment I. Regions were drawn on the MRI data which had been resliced along the coronal plane at a resolution of 256x256x53 voxels, voxel dimension 1 x 1 x 3 mm. One of these original 2D regions before VOI construction and reslicing is seen in Figure 7c,e.

The original MRI dataset was manually segmented and registered to the PET dataset. Regions were tiled and resliced into the PET volume. The count rate for these VOIs was extracted and corrected for partial volume. Results for these four sets of regions are shown in Table 2. Comparison of corrected values for set A with sets B and C shows that the VOI reslicing and correction techniques successfully correct for partial volume effects in regions bordering a broad surface, as would be expected for regions drawn on the cortical surface. The results also show the limits of the correction techniques. It is seen that the corrected activity values calculated for set D, the VOIs around the 3mm tubes, are considerably lower than the expected 4.6 times the mean concentration in compartment II. This result is due to overestimates of the partial volume calculation caused by resolution limits of the MR data. Recalling that the voxel size of the MR data is 1x1x2 mm, it is not surprising that even a careful manual segmentation could not accu-

rately characterize this object. The cross section of a 3 mm tube in a coronal orientation is 7.07 mm^2 whereas the closest binary segmentation of the long axis of the tube in the transaxial orientation voxelized MRI data could choose either a 6 or 8 mm^2 cross section over two slices. Either choice results in over a 15% segmentation error.

The effect of registration errors in the partial volume correction and PET quantification is demonstrated in Figure 8. To obtain these values, the PET-MRI registration matrix was permuted by a translation of ± 4 mm in 1 mm steps along the X-axis in PET space. For each increment in translation offset, a new set of resliced VOIs and partial volume parameters were calculated. Average values of corrected counts were calculated for the four VOI sets in each registration position. The results underscore the importance of accurate registration. For these data, translational registration errors of just 2 mm could produce quantification errors of up to 23%.

4.0 Concluding Remarks

The reported technique for specifying and analyzing VOIs on PET datasets demonstrates an approach for analyzing complex 3D datasets using common 2D interfaces. Navigation through the dataset to find a desired anatomical structure can be greatly simplified using a registered MRI anatomical volume showing multiple simultaneous oblique sections and volume renderings of the data. Because most clinicians can readily identify specific sulci from high-quality renderings of the cortical surface, a crucial step in quickly identifying sulci in 2D sectional data is providing a feedback mechanism between the renderings and the section data. Once identified, 3D VOIs may be specified on the anatomical datasets efficiently in an X-Windows environment by drawing a stack of 2D regions subsequently tiled together to form a VOI surface model. The voxel-independent description of the VOIs allows a quantitative analysis in the observation space of the PET scanner for characterization of both VOI radiotracer activity and statistical properties.

Results obtained from typical brain analyses indicate that the stack of regions defining a VOI may be drawn on slices oriented at the oblique slicing direction which best allows visualization of the desired anatomy's cross-section. A 3 mm slicing separation appears sufficient to capture the salient shape features of regions in the cortex. VOIs drawn using a finer slice separation produced similar quantitative results at the cost of increased manual intervention.

The registration and segmentation steps are seen to be crucial preprocessing steps in the VOI analysis. An accurate segmentation of brain from non-brain structures is needed for PET partial volume corrections, for high-quality surface renderings and for automated registration routines. Phantom analysis results imply that registration between PET and MRI datasets must be achieved to an accuracy greater than 2 mm. Our experiences show that this level of accuracy is difficult to obtain using purely manual techniques. However, by combining manual with automated registration techniques, we are able to obtain reliable registration with minimal manual burden. The manual

portion of the segmentation and registration process has the additional advantage in that quality control can be visually verified by a trained clinician.

Use of 0.5 T MRI data at a voxel resolution of 1 x 1 x 2 mm has the current limitation in our laboratory that the brain grey and white matter cannot be reliably segmented. This limits the extent for which partial volume effects can be corrected. Phantom studies indicate that even if perfect segmentation could be obtained at the resolution of the MRI data, accurate partial volume correction is difficult with an object as small as a 3 mm tube. Correction for this object is a more stringent requirement than the continuous 5-7mm sheet of grey matter, but phantom studies imaging a more realistic brain phantom are warranted.

5.0 Acknowledgment

The authors wish to thank Tony Vuletich for his technical support in the construction of the validation phantom and both Roger Woods and Uwe Pietrzyk, who were extremely helpful in providing their image registration software. This work was supported in part by the Director, Office of Energy Research, Office of Health and Environmental Research, Medical Applications and Biophysical Research Division of the U.S. Department of Energy under contract No. DE-AC03-76SF00098 and in part by the U.S. Department of Health and Human Services under grants HL25840 , AG12435 and AG05890.

6.0 References

[1] C. C. Meltzer, R. N. Bryan, H. H. Holcomb, A. W. Kimball, H. S. Mayberg, B. Sadzot, J. P. Leal, H. N. Wagner, Jr., and J. J. Frost. Anatomical localization for PET using MR imaging. *J Comput Assist Tomogr*, 14(3):418–426, May-June 1990.

[2] S. C. Strother, J. R. Anderson, X. Xu, J. Liow, D. C. Bonar, and D. A. Rottenberg. Quantitative comparisons of image registration techniques based on high-resolution MRI of the brain. *J Comput Assist Tomogr*, 18(6):954–962, 1994.

[3] U. Pietrzyk, K. Herholz, G. Fink, A. Jacubs, R. Mielke, I. Slansky, M. Wurker, and W. Heiss. An interactive technique for three-dimensional image registration: Validation for PET, SPECT, MRI and CT brain studies. *J Nucl Med*, 35(12):2011–2018, Dec 1994.

[4] R. P. Woods, J. C. Mazziota, and S. R. Cherry. MR-PET registration with automated algorithm. *J Comput Assist Tomogr*, 17(4):536–546, 1993.

[5] C. A. Pelizzari, G. T. Y. Chen, D. R. Spelbring, R. R. Weichselbaum, and C. T. Chen. Accurate three-dimensional registration of CT, PET, and/or MR images of the brain. *J Comput Assist Tomogr*, 13:20–26, 1989.

[6] U. Pietrzyk. A rapid three-dimensional visualisation technique to evaluate function in relation with anatomy of the

human cortex. In *Conference Record of the 1993 IEEE Nuclear Science Symposium and Medical Imaging Conference*, volume 3, pages 1810–1812, 1993.

[7] R. A. Peters III. Software for 2d and 3d mathematical morphology. Technical report, Air Force Office of Scientific Research, 1991.

[8] E. A. Hoffman, D. Gnanaprakasam, K. B. Gupta, J. D. Hoford, S. D. Kugelmass, and R. S. Kulawiec. VIDA: An environment for multidimensional image display and analysis. *Communications ACM*, 20:693–702, 1992.

[9] G. J. Klein, B. W. Reutter, R. H. Huesman, P. G. Coxson, and T. F. Budinger. Volume-of-interest specification on arbitrarily resliced volume datasets. In E. Hoffman, editor, *Medical Imaging 1995: Physiology and Function from Multidimensional Images*, volume Proc. SPIE 2433, pages 214–223, 1995.

[10] J. Boissannat and B. Geiger. Three-dimensional reconstruction of complex shapes based on the Delaunay triangulation. Technical report, INRIA Sophia-Antipolis, 1992.

[11] B. Baumgart. Winged-edge polyhedron representation. Technical report, Stanford, 1972.

[12] J. Wernecke. *The Inventor Mentor: Programming Object-Oriented 3D Graphics with Open Inventor, release 2.* Addison-Wesley, Reading, Mass., 1994.

[13] R. H. Huesman. A fast new algorithm for the evaluation of regions of interest and statistical uncertainty in computed tomography. *Phys Med Biol*, 25(5):543–552, 1984.

[14] R. E. Carson, Y. Yan, M. E. Daube-Witherspoon, N. Freedman, S. L. Bacharach, and P. Herscovitch. An approximation formula for the variance of PET region-of-interest values. *IEEE Trans Med Imag*, 12(2):240–250, Jun 1993.

[15] C. C. Meltzer, J. P. Leal, H. S. Mayberg, H. N. Wagner, Jr, and J. J. Frost. Correction of PET data for partial volume effects in human cerebral cortex by MR imaging. *J Comput Assist Tomogr*, 14(4):561–570, 1990.

[16] H. W. Muller-Gartner, J. M. Links, J. L. Prince, R. N. Bryan, E. McVeigh, J. P. Leal, C. Davatzikos, and J. J. Frost. Measurement of radiotracer concentration in brain gray matter using positron emission tomography: MRI-based correction for partial volume effects. *J Cereb Blood Flow Metab*, 12(4):571–583, 1992.

[17] K. Wienhard, M. Dahlbom, L. Eriksson, C. Michel, T. Bruckbauer, U. Pietrzyk, and W. Heiss. The ECAT EXACT HR: Performance of a new high resolution positron scanner. *J Comput Assist Tomogr*, 18(1):110–118, 1994.

[18] W. J. Jagust, J. P. Seab, R. H. Huesman, P. E. Valk, C. A. Mathis, B. R. Reed, P. G. Coxson, and T. F. Budinger. Diminished glucose transport in Alzheimer's disease: Dynamic PET studies. *J Cereb Blood Flow Metab*, 11:323–330, 1991.

[19] M. E. Phelps, S. C. Huang, E. J. Hoffman, C. Selin, L. Sokoloff, and D. E. Kuhl. Tomographic measurement of local cerebral glucose metabolic rate in humans with (F-18)2-fluoro-2-deoxy-d-glucose: Validation of method. *Ann Neurol*, 6:371–388, 1979.

TABLE 1. Registration Comparison - Automatic and Manual Techniques

	Auto vs Manual 1	**Auto vs Manual 2**	**Manual 1 vs Manual 2**
Average Rotational Difference (deg)	2.62	2.19	3.07
Rotational Difference Range	0.15-4.56	0.25-5.43	0.41-7.54
Average Translation Difference (mm)	1.95	3.31	3.12
Translation Difference Range	1.50-2.79	1.06-5.40	1.29-4.91

TABLE 2. Phantom Partial Volume Correction Results

Region Label	Relative Concentration	VOI Activity (counts/cc/sec)	Partial Volume (fraction)	Corrected Counts (counts/cc/sec)
A1	1	675	1.000	674
A2	1	663	1.000	663
A3	1	623	1.000	623
B1	1	362	0.590	613
B2	1	302	0.460	657
B3	1	278	0.422	660
C1	1	431	0.636	677
C2	1	443	0.692	640
C3	1	493	0.726	680
D1	4.6	279	0.119	2393
D2	4.6	272	0.140	1964
D3	4.6	232	0.107	2488
D4	4.6	308	0.158	1952

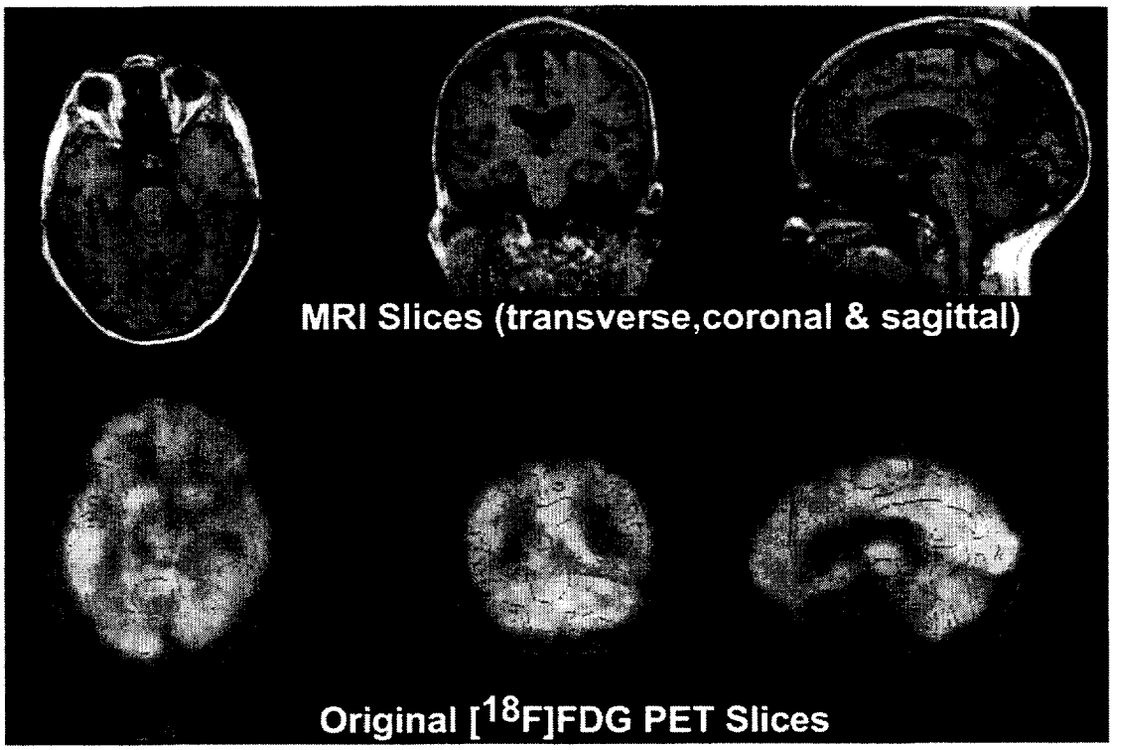

Figure 1. Manual Segmentation. FDG PET data are quickly registered to the MRI dataset using this manual interface. The registered PET data are thresholded and used as a binary mask to automatically segment the brain from non-brain structures in the MRI. Once the segmentation is obtained, the registration is refined using automated techniques.

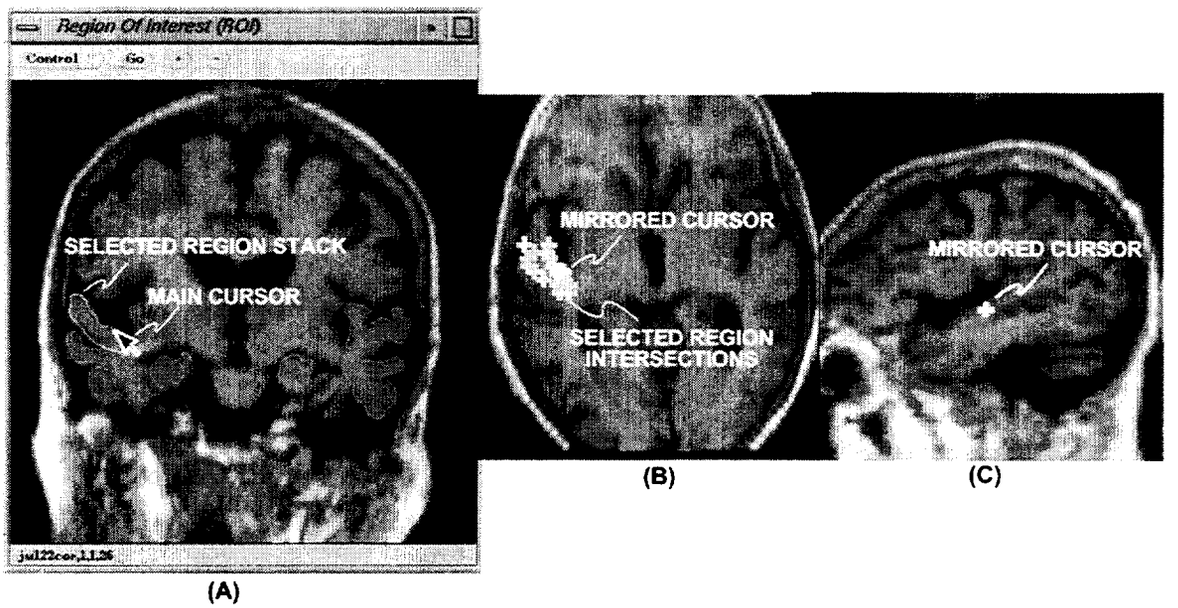

Figure 2. Region Drawing Environment. A main drawing window (A) is used to draw 2D regions. The main window cursor position is mirrored in real-time on auxiliary views (B,C) as a projected 3D crosshair cursor to aid visualization of the 3D anatomy. Intersections of selected region stacks with the auxiliary planes (B) give the user intuition of the 3D shape of the resulting VOI.

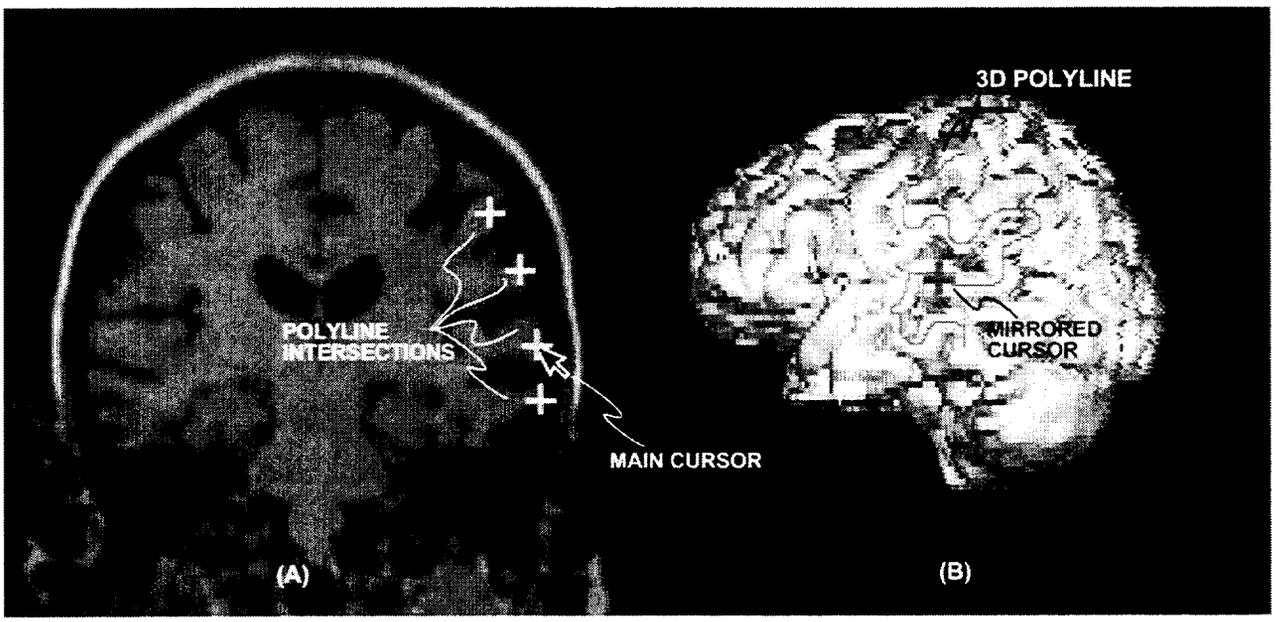

Figure 3. Volume Rendering-Based Navigation. 3D positional information is recorded for each pixel in the volume rendering (B), allowing an interface tying together 2D sectional (A) with rendered information. Intersections of a polyline drawn on the rendering are shown as crosses on the 2D view. Position of the cursor in the 2D view is reflected in the rendering in real time.

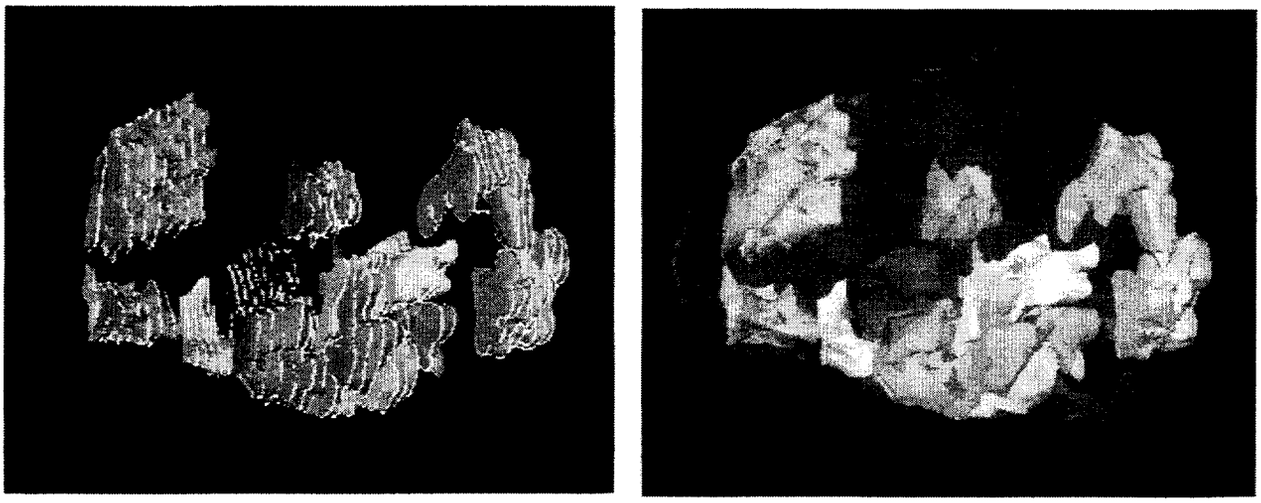

(A) (B)

Figure 4. Volumes of Interest. 3D Volumes of Interest are created by tiling stacks of 2D contours. Contours in (A) are overlaid on the resulting VOI surfaces. A typical set of VOIs drawn for a brain study is seen in (B) in a schematic rendering of the cortical surface

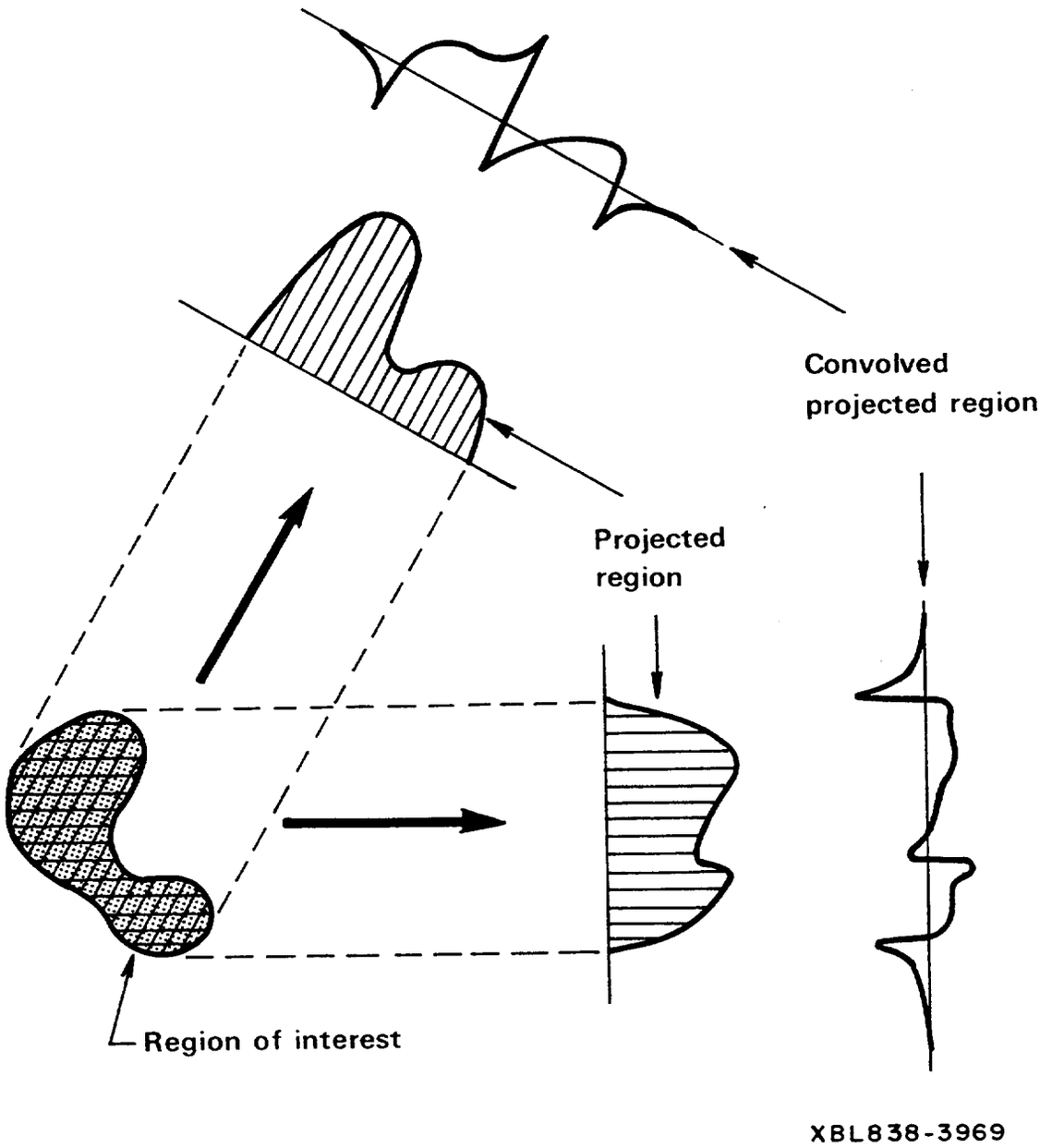

Figure 5. PET Statistical Quantitation. Activity from a VOI slice is evaluated by projecting the uniformly weighted region at each angle. The projected region is convolved, and an vector inner product is formed with the raw tomographic data set. Activity from all slices of the VOI are summed to obtain the composite activity and uncertainty at a single time point for that volume.

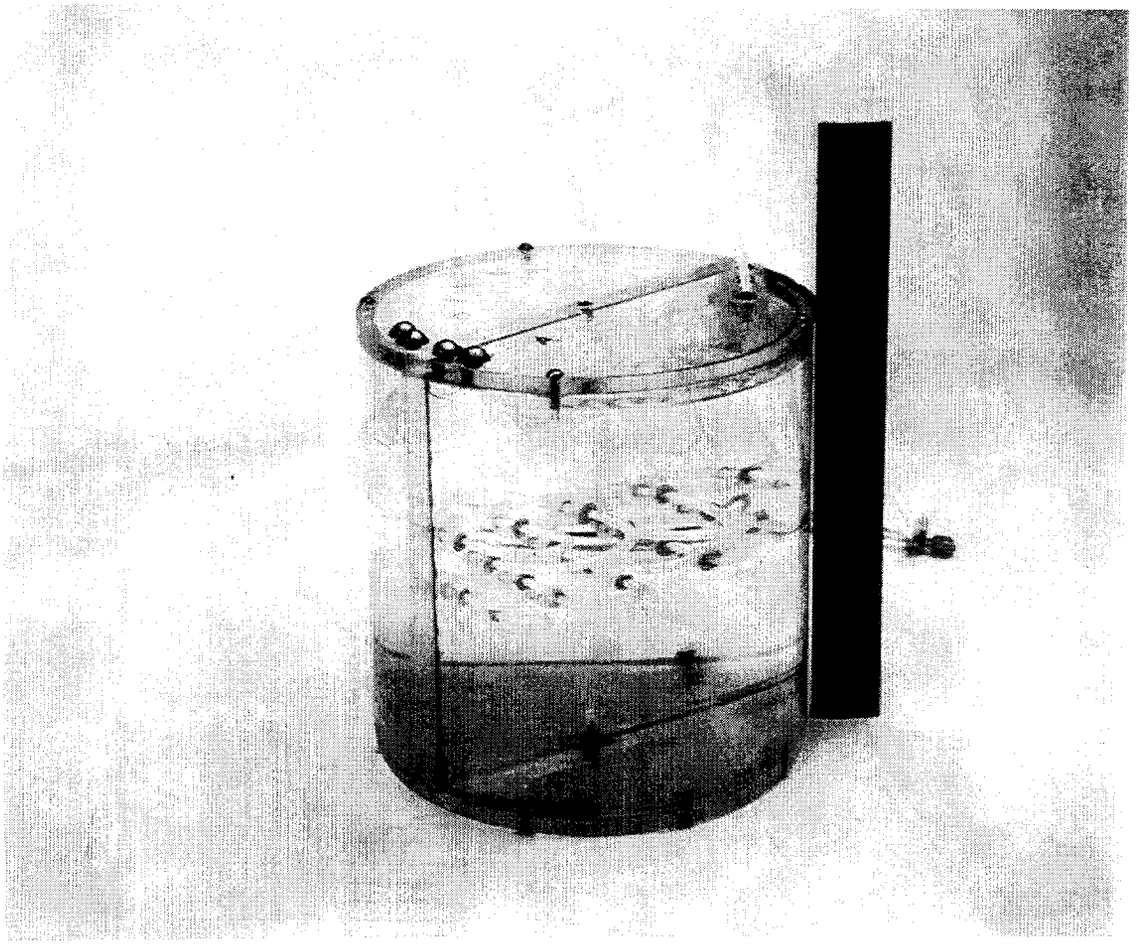

Figure 6. Three Compartment Cylindrical Phantom. A 3 mm tube passing through two halves of the plexiglass cylindrical phantom allows validation of atrophy correction and region placement between PET and resliced MRI images.

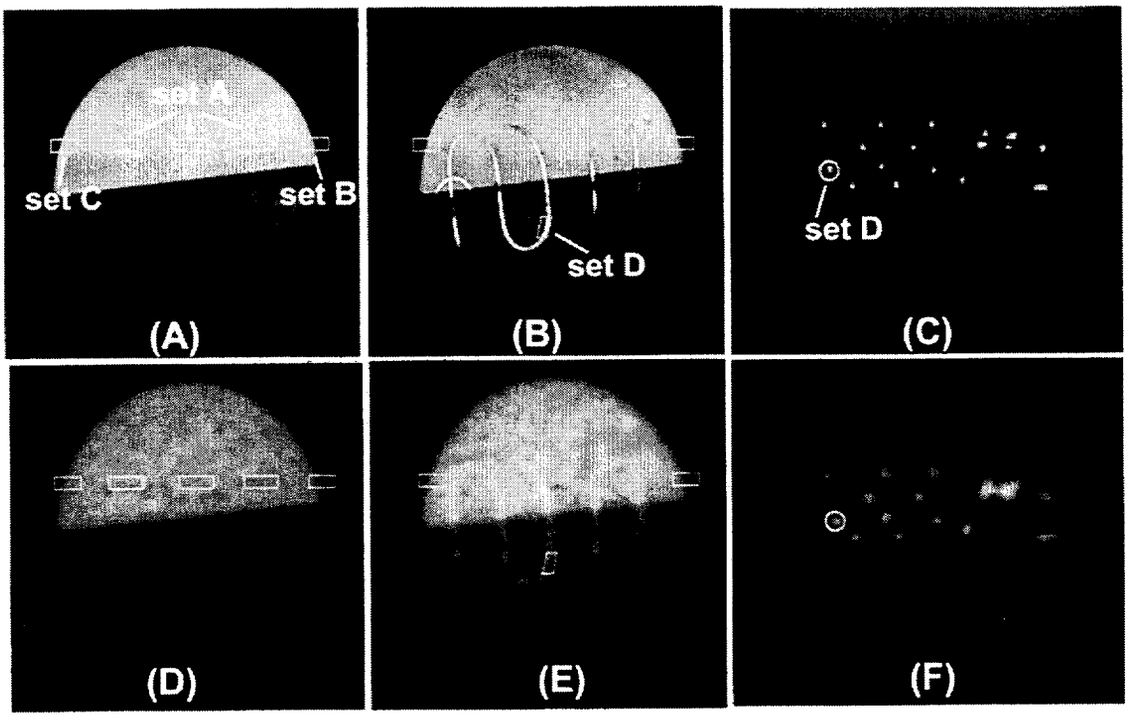

Figure 7. MRI and PET slices (transaxial: A,B,D,E and coronal: C,F) through the three-compartment cylindrical phantom used for validation of VOI reslicing and partial volume correction. Four sets of VOIs were drawn on the coronally resliced MRI data of the phantom and were used to quantify activity in the PET dataset. One of the original 2D regions comprising a VOI is seen in the coronal slices. Intersections of some of the other VOIs are shown in the transaxial slices.

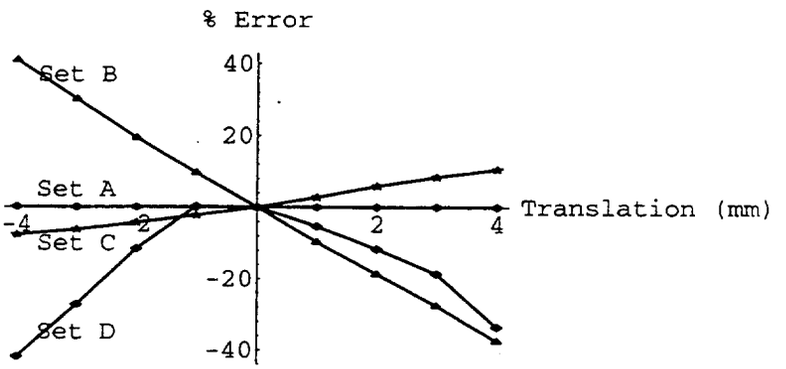

Figure 8. Misregistration Effects. Average percent quantitation differences induced by misregistration errors in the cylindrical phantom. Results show that translational misregistrations of just 2 mm can produce large quantitation errors.